p53 Knock Out Mice Enhances Anxiety- and Depression-Like Behaviors through an Increase of Glutamate, Calcium, and Cytokine-Mediated Cell Death Signals

In Jun Yeo
Chungbuk National University
Ji Eun Yu
Chungbuk National University
Sung Sik Yoo
Chungbuk National University
Jaesuk Yun
Chungbuk National University
Dong Ju Son
Chungbuk National University
Dong-Young Choi
Yeungnam University
Sang-Bae Han
Chungbuk National University
Jin Tae Hong (jinthong@chungbuk.ac.kr)
Chungbuk National University

Research Article

Keywords: p53, BDNF, glutamate, anxiety, depression

Posted Date: October 6th, 2021

DOI: https://doi.org/10.21203/rs.3.rs-929317/v1

Abstract

Extensive epidemiological evidence indicates that patients with certain cancers have a lower probability of developing some types of neurodegenerative diseases (ND) and mood disorders and vice versa. These inverse comorbidities may be associated with several different molecular processes. p53, is a potentially responsible for regulating the development of ND, mood disorders as well as cancers. To investigate whether the tumor suppressor p53 may be associated with ND development, we studied the behavioral changes in p53 knockout ($p53^{-/-}$) mice and possible action mechanisms. Increased anxiety-like but not depression-like behaviors were displayed in $p53^{-/-}$ mice without impaired motor activities under the non-chronic unpredictable mild stress condition. However, in the $p53^{-/-}$ mice, more anxiety-like and depression-like behaviors were observed in the chronic unpredictable mild stress (CUMS) condition. Our mechanism studies showed that brain-derived neurotrophic factor (BDNF) protein was significantly downregulated, but glutamate levels were significantly increased in the prefrontal cortex of $p53^{-/-}$ mice. Further analyses showed that the $p53^{-/-}$ mice caused more stress-induced nerve damage as a result of an increase in intracellular calcium levels and N-methyl D-aspartate receptor subtype 2B (NMDAR2B) expression. Treatment with corticosterone (mimics CUMS *in vitro*) increased glutamate levels, NMDAR2B expression, and calcium levels, and these levels were elevated by co-treatment with pifithrin-α (p53 inhibitor) in PC12 cells. Cell death and cell death-mediated signals (p-p38, p-JNK and caspase-3) were upregulated, but neuroprotective signals (BDNF p-Akt, p-ERK and p-CREB) were downregulated in $p53^{-/-}$ mice, and corticoid and/or pifithrin-α treated PC12 cells. These data indicate that p53 may be an important preventive factor against depression and anxiety, and thus suggests a possible correlation between cancer and anxiety/depression development.

Running title: Deficiency of p53 enhances mental disorder

Introduction

Extensive epidemiological evidence indicates that patients with certain cancers have a lower probability of developing some types of neurodegenerative diseases (NDs) such as Alzheimer's disease (AD), Parkinson's disease (PD) and schizophrenia (SCZ), and vice versa[1]. These inverse comorbidities may be associated with several different molecular processes. A transcriptomic meta-analysis of three ND types and three cancer types (lung, prostate, and colorectal) demonstrated the inverse comorbidities, and significant overlapping genes were found to be upregulated in NDs but downregulated in cancers. They were also found to be downregulated in NDs but upregulated in cancers[2–5]. One of these molecules, p53, is potentially responsible for regulating the development of NDs and cancer[6–8].

Several studies have also demonstrated that p53 could be involved in complex molecular interactions putatively associated with the inverse correlation between cancer and AD[6,9]. Moreover, p53 at the transcriptional level was recently shown to upregulate parkin, a gene responsible for the development of PD[10]. The upregulation of parkin levels could, in turn, contribute to the activation of p53 at the

transcriptional level, which could explain, at least in part, the increased cellular apoptotic commitment in cerebral cancer[11]. Previous studies have demonstrated that the inhibition of p53 could be an important indicator for the treatment of neuropathic symptoms[12,13].

Although many studies have supported the correlation among p53, tumor suppressor molecules, and ND susceptibility, evidence of a causal relationship is still lacking. The overexpression of the p53 gene has been shown to lead to excessive neuronal death and impaired neural function[14]. In patients with SCZ, p53 activation can enhance apoptosis[15,16]. Therefore, p53 hyper-activation may enhance tumor surveillance with higher neuronal apoptosis, which impairs psychiatric function. In addition, transcriptional regulation may help to explain the potentially causal relationship between tumor suppressor gene activity and SCZ[17]. It was also reported that anti-anxiety and anti-depressant drugs, such as midazolam and amitriptyline, have shown anti-cancer effects through p53-dependent cell cycle arrest and therefore, the induction of apoptosis[18]. However, a causal relationship between anxiety/depression and cancer, and the role of p53 in this relationship has not yet been elucidated[19]. Therefore, we investigated the effects of p53 on anxiety and depression using p53 knockout mice treated with/without chronic unpredictable mild stress (CUMS) and possible mechanisms[20].

Results

$p53^{-/-}$ mice show anxiety and depression under CUMS

We evaluated the effects of p53 knockout on anxiety-related and depression-related behaviors in $p53^{-/-}$ mice. CUMS was performed as described[21], and a behavioral test was shown in Figure 1A. In the anxiety test, $p53^{-/-}$ mice performed significantly worse on the central zone time (%), entries, and distance (cm) in the open field test (OFT) after CUMS (Figure 1B). The performance of $p53^{-/-}$ mice in the elevated zero maze (EZM), which also evaluates anxiety-like behaviors, was significantly lower than that of wild-type (WT) mice in time (%) and entries in the open arm after CUMS (Figure 1C). Using the tail suspension test (TST) and forced swimming test (FST), depression-like behaviors were demonstrated through the increased immobility of $p53^{-/-}$ mice after CUMS compared to WT mice (Figure 1D and E). Together, these findings indicate that a deficiency of p53 increases higher anxiety and depression.

p53 deficiency under CUMS increases calcium and glutamate levels in PFC

After the behavioral tests, we collected brain tissues from mice, and measured calcium levels in the prefrontal cortex (PFC). A significant increase of calcium in the $p53^{-/-}$ PFC after CUMS compared to WT mice was shown by Alizarin Red S staining (Figure 2A). We next investigated the expression of calcium related signal proteins; calpain-1 and calpain-2. Calpains are mediators of calcium and neuroprotection in nerves, especially calpain-1, which is involved in neuroprotection, whereas calpain-2 facilitates neurodegeneration[22]. The mRNA and protein expression of calpain-1 was much significantly increased in WT mice after CUMS compared to $p53^{-/-}$ mice after CUMS, but that of calpain-2 was significantly

increased in p53$^{-/-}$ mice after CUMS compared to WT mice after CUMS (Figure 2B and 2C). Next, we measured the calcium-related neurotransmitter; glutamate by HPLC. Significantly increased levels of glutamate were found in the p53$^{-/-}$ mice PFC after CUMS compared to WT mice PFC after CUMS (Figure 2D). N-methyl D-aspartate receptor subtype 2A (NMDAR2A) and NMDAR2B are subtype of calcium-permeable ionotropic glutamate receptors in neurons. During pathological conditions, increased glutamate activate NMDAR and result in increased calcium influx and neuronal death by preferential activation of NMDAR; NMDR2A is related to neuronal survival, whereas NMDAR2B is related to neuronal death signaling[23]. Recent studies suggest that NMDRAR2A deficiency cause schizophrenia-like phenotype[24,25]. Thus, we examined NMDAR2A and NMDAR2B expression by PCR and Western blot analyses in mice. NMDAR2B expression significantly increased in p53$^{-/-}$ mice compared to WT mice PFC after CUMS, whereas the expression of NMDAR2A was significantly much increased in WT mice compared to p53$^{-/-}$ mice PFC after CUMS (Figure 2E and 2F). There were no significant differences in the calpain-1, calpain-2, NMDAR2A, and NMDAR2B expressions between p53$^{-/-}$ and WT mice HP after CUMS (Supplementary Figure 1). These results suggest that significantly increased glutamate secretion and calcium influx after CUMS in neurons was associated with calpain-2 and NMDAR2B pathway in p53$^{-/-}$ mice PFC, and effects may be involved in neuronal cell death.

p53 deficiency under CUMS leads to neuronal cell death and activates related signals

The influx of calcium into cells is an important signal for cell death. We examined whether these differential calcium and glutamate levels could result in cell death. Significantly decreased neuronal cell number and increased cleaved caspase-3-stained areas were observed via cresyl violet staining (Figure 3A) and IHC (Figure 3B), respectively, in p53$^{-/-}$ mice PFC after CUMS. However, there was no significant difference in the neuronal cell death between p53$^{-/-}$ mice HP and WT mice HP (Supplementary Figure 2). We evaluated the expression changes in the cell death relevant indicators through PCR and Western blot analyses. In line with the cell death pattern, the significantly increased expression of the caspase-3 (Figure 4A) gene and cleaved caspase-3 protein was found (Figure 4B) in p53$^{-/-}$ mice PFC after CUMS. Cell death-related protein (p-p38 and p-JNK) expression was also significantly increased in p53$^{-/-}$ mice PFC after CUMS (Figure 4C), whereas the expression of neuroprotective indicators (Wip1, brain-derived neurotrophic factor (BDNF), p-Akt, p-ERK, and p-CREB) was significantly decreased in p53$^{-/-}$ mice PFC after CUMS compared to WT mice PFC after CUMS (Figure 4D, 4E, and 4F). There were no significant differences in the expression of these signals in p53$^{-/-}$ and WT mice HP (Supplementary Figure 3). These results indicate that p53 deficiency increase cell death through upregulating cell death signals and downregulating neuroprotective signals under CUMS.

P53 Deficiency Under Cums Induces Neuroinflammation

To determine whether the cell death effect in p53$^{-/-}$ mice is associated with the activation of astrocytes and microglia, the expression levels of GFAP (astrocyte activation marker) and Iba-1 (microglia activation

marker) were detected through Western blot. A significant increase in GFAP and Iba-1 expression was observed (Figure 5A). Next, we measured the release of inflammatory cytokines (IL-1β, IL-6, and TNF-α). Significant increases in the gene mRNA expression of inflammatory cytokines in $p53^{-/-}$ mice PFC after CUMS (Figure 5B). Higher cytokines concentration in $p53^{-/-}$ mice serum after CUMS were also observed compared to WT mice after CUMS (Figure 5C). However, there were no significant differences between $p53^{-/-}$ mice HP after CUMS and WT mice HP in the activation of microglia and astrocytes as well as cytokines releases (Supplementary Figure 4). These data indicate that a deficiency of p53 in mice under CUMS causes neuroinflammatory activity.

Effects of p53 inhibition on cell survival, glutamate/calcium levels, and cell death signals

An *in vivo* study demonstrated that p53 deficiency increases cell death by increase of glutamate release and calcium influx as well as cytokine release. To mimic the CUMS model in cells, PC12 cells were treated for 24 hours upon stimulation with corticosterone (CORT; 100 μM) with/without the inhibition of p53 by pifithrin-α (PTF-α; 100 μM). We observed that calcium levels were increased in CORT-treated PC12 cells via Alizarin Red S staining (red intensity increased) and further increased by the combination treatment of cortisone and PTF-α, but the cell number was decreased by CORT treatment and further decreased by the combination treatment (Figure 6A). The expression of p53 was downregulated by CORT treatment and further decreased by PTF-α treatment. The expression of the calcium related calpain-1 -2 mRNA and protein were significantly increased by CORT treatment, but it was decreased by a combination treatment, whereas significant increase was observed in the calpain-2 by a combination treatment (Figure 6B and 6C). Next, we measured the glutamate levels in the supernatant of PC12 cells by HPLC. Glutamate levels were significantly increased by CORT treatment and further increased by the combination treatment (Figure 6D). Glutamate receptor subtype gene (NMDAR2A and 2B) and protein expression were detected. The expression of NMDAR2A was increased by CORT treatment, but decreased by the combination treatment, whereas that of NMDAR2B was increased by CORT treatment and further increased by the combination treatment (Figure 6E and 6F). We next investigated the cell death signal pathway. Caspase-3 gene mRNA expression increased significantly after CORT treatment, but CORT treatment with/without PTF-α was not significantly different (Figure 7A), but the expression of cleaved caspase-3 was significantly increased by CORT treatment and further increased by PTF-α (Figure 7B). The expression of cell death signal proteins (p-p38 and p-JNK) were also significantly increased by CORT treatment and further increased by the combination treatment with PTF-α (Figure 7C). Conversely, CORT-induced the expression of neuroprotective signal proteins (Wip1, BDNF, p-Akt, p-ERK, and p-CREB) was increased, but was decreased by the combination treatment with CORT and PTF-α (Figure 7D, 7E, and 7F). Inflammatory cytokine (IL-1β, IL-6, and TNF-α) mRNA and release levels were significantly increased by CORT treatment and further increased by the combination treatment with PTF-α (Figure 8A and 8B).

Discussion

Although several studies have demonstrated the inverse correlation between p53, a tumor suppressor gene, and ND susceptibility, a causal relationship between anxiety/depression and cancer has not yet

been reported[11,14]. Several studies have demonstrated that p53 may serves to maintain important neuronal systems and synaptic functions[26,27]. It is also noteworthy that the absence of p53 activates the neuronal cell death pathway, which can lead to nerve damage in AD, PD, and SCZ[15,28,29]. Therefore, we speculated that the absence of p53 could worsen anxiety and depression. To solve out this speculation, we performed anxiety and depression behavioral tests in $p53^{-/-}$ mice. Our data showed that the $p53^{-/-}$ mice enhanced anxiety and depression behaviors after CUMS. Similar to our data, a recent study showed increased anxiety and depressive behaviors in WT p53-induced phosphatase 1 (wip1)-deficient mice[21]. However, the mechanism how deficiency of p53 enhances anxiety and depression remains unclear.

Glutamate is ubiquitous within the CNS and has been shown to play important roles in many brain processes, including neurodevelopment (e.g., differentiation, migration, and survival) and learning (e.g., long-term potentiation and depression). However, higher levels of glutamate cause excitotoxicity associated with acute neurodegeneration (e.g., cerebral ischemia and traumatic brain injury), chronic neurodegeneration (e.g., HD and AD), and anxiety disorders[30]. The normal influx of calcium is also important for maintenance of neuron functions. However, chronic calcium influx is also associated with specific neurotoxic events. A study showed that intracellular calcium concentrations are increased in patients with bipolar disorder and depression[31]. Moreover, calcium channel blockers prevent calcium influx, and is used as an antidepressant. A study also showed that calcium channel blockers such as verapamil, diltiazem, and flunarizine are effective at reducing anxiety-related behaviors[32]. Calcium channel blockers has been also proven effective at reducing depressive-like symptoms in both animal and human studies[32–34]. Our results showed an increase in the release of glutamate and calcium in $p53^{-/-}$ mice brains after CUMS. This increase of glutamate and calcium causes was associated neuronal cell death. The type of glutamate receptor (NMDAR2A or 2B) determines neuronal cell death or neuroprotective activation[35]. While NMDAR2A is associated with neuroprotection, NMDAR2B is associated with apoptosis, and both receptors increase calcium influx[36]. In addition, calpain, a calcium-dependent protein, also functions differentially; calpain-1 is related to neuroprotection, while calpain-2 is related to cell death[37,38]. In the present study, we found that with glutamate release and calcium influx, the expression of NMDAR2B and calpain-2 was increased, while the expression of NMDAR2A and calpain-1 was decreased in the $p53^{-/-}$ mice brain after CUMS. We also found that cell death was increased in mice brains after CUMS and in CORT-treated PC12 cells, and PC12 cell death was further increased by the combination treatment of CORT and p53 inhibitor (PTF-α). These results indicate that the increase of glutamate and calcium levels through the differential expression of NMDAR2 and calpain may be associated with cell death in $p53^{-/-}$ mice brains after CUMS and in CORT + PTF-α-treated PC12 cells. These results further indicate that glutamate- and calcium-dependent neuronal cell death could enhance anxiety and depression in $p53^{-/-}$ mice.

Furthermore, calcium and glutamate have been associated with cell death signals (cleaved caspase-3, p-p38, and p-JNK) and neuroprotective factors (Wip1, BDNF, p-Akt, p-ERK, and p-CREB)[39,40]. Our animal study demonstrating the absence of p53 under stress increased cell death signals but decreased

neuroprotective signals. Moreover, in cultured PC12 cells, CORT treatment increased cell death signals, which were further increased by PTF-α treatment. CORT-induced upregulated neuroprotective signals were inhibited by PTF-α. The elevation of glutamate and calcium could increase the release of cytokines[30]. In our study, we found that in $p53^{-/-}$ mice brains after CUMS and in CORT-treated PC12 cells, IL-1β, IL-6, and TNF-α was significantly elevated, and PTF-α cotreatment further released these cytokines. It is noteworthy that neurons are vulnerable to inflammatory attacks[41]. Considering the significant involvement of inflammatory cytokines in patients with NDs, such as AD, PD, and HD[42], elevation of these cytokine elevations could worsen anxiety and depression in $p53^{-/-}$ mice after CUMS. Therefore, our data demonstrated that in p53 deficient mice and CORT-treated PC12 cells, the activation of cell death signals and enhanced cytokine release resulted in neuronal cell death.

Conclusively, we found that a deficiency of p53 could increase anxiety and depression by glutamate-, calcium- and cytokine- dependent neuronal cell death. p53 is a tumor suppressor gene, and it inhibits the development of many cancers, such as breast, gastric, and lung cancer[43]. Therefore, results suggest that p53 deficiency induces anxiety and depression, and these effects are inversely related to the p53-dependent inhibition of cancer development.

Methods

All methods carried out in accordance with relevant guidelines and regulations.

Animals

The $p53^{-/-}$Tg mice (C57BL/6J-$Trp53^{em1hwl}$/Korl; KO created by TALEN-induced NHEJ) were thankfullygiven from the MISP (Osong, Korea). The non-transgenic and $p53^{-/-}$Tg mice used were C57BL/6 mice. The mice were housed and bred under specific pathogen-free conditions at the Laboratory Animal Research Center of the Chungbuk National University, Korea. All experimental procedures in the present study were approved by the IACUC of Chungbuk National University (approval number: CBNUA-1277-19-01) and performed by ARRIVE guidelines. The mice were maintained in a room with a constant temperature of 22 ± 1 °C, relative humidity of 55 ± 10%, and under a 12/12-h light/dark cycle. Standard rodent chow (Samyang, Gapyeong, Korea) and purified tap water were available ad libitum.

CUMS procedure

CUMS was performed as described in the references[21]. Briefly, as control mice were socially housed and undisturbed, mice for CUMS were singly housed and daily experienced a random stimulus of 10 for a specified duration. Stimuli were cold water swimming (13±1 °C, 5 min) (A), warm water swimming (37±2 °C, 5 min) (B), moist bedding (8 h) (C), cage tilt (45°, 8 h) (D), cage shaking (180 rpm, 10 min) (E), tail inch (1 cm from the tail end, 1 min) (F), food deprivation (12 h) (G), water deprivation (12 h) (H), overnight illumination (12 h) (I) and no stress (24 h) (J). To examine the effect of CUMS on animals, OFT was

weekly performed starting from the beginning, while EZM, TST as well as FST were performed at the beginning and end of the CUMS procedure.

Behavioral test

The 8-week-old $p53^{-/-}$& WT mice were tested. Mice take adaptation time for a week. Each behavioral test run 24 h interval.

Open Field Test

OFT was performed as described in the references[21]. Briefly, animals were placed in an open arena and recorded by a video camera for 5 min. Travel distance, turn angle, entries in the peripheral zone, entries in the central zone and percentage of time spent in the central zone were automatically analyzed by SMART-LD program (Panlab). Entries in the peripheral zone and the central zone, as well as the percentage of time spent in the central zone indicated the anxiety-like behaviors.

Elevated Zero Maze

EZM was performed as described in the references[21]. Briefly, animals were placed in anannular platform elevated above the floor and recordedby a video camera for 5 min. Data were automaticallyanalyzed by SMART-LD program (Panlab).The travel distanceand turn angle in the closed arms respectively indicatedthe locomotor and non-locomotor movements of the body,while the travel distance and turn angle in the open armsindicated the exploratory behaviors. Entries in the closedarms and open arms, as well as the percentage of timespent in the open arms indicated the anxiety-like behaviors.

Tail suspension test

TST was performed as described in the references[21].Briefly, animals were suspendedabove the floor and recorded by a video camera for6 min. The duration of immobile behavior was manuallymeasured blinding to the treatment. The increase ofimmobility indicated the depression-like behavior.

Forced Swim Test

FST was performed as described in the references[21].Briefly, animals were placed in a cylindercontaining water and recorded by a video camera for6 min. The duration of climbing and immobile behaviorswas manually measured in the first 2 min and last4 min respectively blinding to the treatment. The increaseof immobility and decrease of climbing both indicated thedepression-like behaviors.

Brain collection and preservation

After the behavioral tests, mice were perfused with phosphate-buffered saline (PBS, pH 7.4) under inhaled CO_2 anesthetization. The brains were immediately removed from the skulls and divided into the left brain

and right brain. One stored at − 80 °C and the other fixed in 4% paraformaldehyde for 48 h at 4 °C and transferred to 30% sucrose solutions.

Immunohistochemical staining

After being transferred to 30% sucrose solutions, brains were cut into 10μm sections by using a cryostat microtome (Leica CM 1850; Leica Microsystems, Seoul, Korea). After two washes in PBS (pH 7.4) for 10 min each, endogenous peroxidase activity was quenched by incubating the samples in 3% hydrogen peroxide in PBS for 20 min, and then two washes in PBS for 10 min each. The brain sections were blocked for 1 h in 1% bovine serum albumin (BSA) solution and incubated overnight at 4 °C with a rabbit polyclonal antibody against cleaved caspase-3 (1:100; Cell Signaling Technology,Danvers, MA, USA). After incubation with the primary antibodies, brain sections were washed three times in PBS for 10 min each. After washing, brain sections were incubated for 1–2 h at room temperature with the biotinylated goat anti-rabbit IgG-horseradish peroxidase (HRP) secondary antibodies (1:1000; Santa Cruz Biotechnology, Inc., Santa Cruz, CA, USA). Brain sections were washed thrice in PBS for 10 min each and visualized by a chromogen DAB (Vector Laboratories) reaction for up to 10 min. Finally, brain sections were dehydrated in ethanol, cleared in xylene, mounted with Permount (Fisher Scientific, Hampton, NH), and evaluated on a light microscope (Microscope Axio Imager.A2, Carl Zeiss, Oberkochen, Germany).

Western blotting

In *in vivo* study, for comparing the expression of protein levels through Western blotting, we selected and used 4 of 10 mice brain from each group. Protein was extract by PRO-PREP™ Protein Extraction Solution (iNtRON Biotechnology, Inc., Seongnam, Korea). An equal amount of total protein (20 μg) was resolved on 8-15% sodium dodecyl sulfate polyacrylamide gel and then transferred to a nitrocellulose membrane (Hybond ECL; Amersham Pharmacia Biotech, Piscataway, NJ, USA). The membranes were blocked for 1 h in 2.5 % skim milk solution and incubated overnight at 4 °C with specific antibodies. To detect target proteins, specific antibodies against calpain-1 (Mybiosource, Inc., San Diego, CA, USA), calpain-2 (Santa Cruz Biotechnology, Inc., Santa Cruz, CA, USA), NMDAR2A (Thermo Fisher Scientific, Waltham, MA, USA), NMDAR2B (Thermo Fisher Scientific, Waltham, MA, USA), p53 (Abcam, Inc., Cambridge, MA, USA), Caspase-3 (Cell Signaling Technology,Danvers, MA, USA), p-p38 (Cell Signaling Technology,Danvers, MA, USA), p38 (Cell Signaling Technology,Danvers, MA, USA), p-JNK (Cell Signaling Technology,Danvers, MA, USA), JNK (Cell Signaling Technology,Danvers, MA, USA), Wip1 (Santa Cruz Biotechnology, Inc., Santa Cruz, CA, USA), BDNF (Arigo biolaboratories,Hsinchu City,Taiwan), p-Akt (Santa Cruz Biotechnology, Inc., Santa Cruz, CA, USA), Akt (Santa Cruz Biotechnology, Inc., Santa Cruz, CA, USA), p-ERK (Cell Signaling Technology,Danvers, MA, USA), ERK (Cell Signaling Technology,Danvers, MA, USA), p-CREB (Cell Signaling Technology,Danvers, MA, USA), CREB (Cell Signaling Technology,Danvers, MA, USA), GFAP (Santa Cruz Biotechnology, Inc., Santa Cruz, CA, USA), Iba-1 (Abcam, Inc., Cambridge, MA, USA), and β-actin (Santa Cruz Biotechnology, Inc., Santa Cruz, CA, USA) were used (1:1000), overnight incubation at 4 °C. The blots were then incubated with the corresponding conjugated goat anti-rabbit or goat anti-mouse or donkey anti-goat IgG-horseradish peroxidase (HRP) (1:5000; Santa Cruz Biotechnology Inc. Santa Cruz,

CA, USA) secondary antibodies, 1 hours 30 min incubation at room temperature. Immunoreactive proteins were detected with an enhanced chemiluminescence Western blotting detection system. The relative density of the protein bands was measured by ImageJ (Wayne Rasband, National Institutes of Health, Bethesda, MD).

Histochemical staining for calcium

Slides were then incubated in 2% Alizarin Red S (Sigma A-5533) pH 4.3 (adjusted with ammonium hydroxide) and blotted to remove excess dye. Slides were then dipped 20 times in acetone, followed by 20 times in acetone-Citrisolv. Slides were then cleared in Citrisolv a mountedslide evaluated on a light microscope (Microscope Axio Imager.A2, Carl Zeiss, Oberkochen, Germany).

Cresyl violet staining

Cresyl violet staining was performed as reported[44]. Frozen hippocampal tissues were cut into 10 μm sections by using cryostat microtome (Leica CM 1850; Leica Microsystems, Seoul, Korea). The pieces of tissues were fixed in 4% paraformaldehyde for 24 h at 4 °C. In order to identify cortical layers and cytoarchitectural features of the isocortical region, the post-fixed tissues were washed with PBS and then transferred to gelatin-coated slides and stained with 0.1% Cresyl violet (10 min). The sections were then washed with distilled water and dehydrated in 50%, 70%, 90%, and 100% ethanol for 2 min in each concentration. The tissues were airdried and immersed in a 1:1 mixture of absolute ethanol and xylene for 1 min. Following removal of the previous solution, the tissues were rinsed with xylene for 5–10 min and mounted with mounting medium (Cytoseal XYL, Thermo Scientific, USA). The matching areas of tissues were photographed at 100xmagnification.

RNA isolation and quantitative real-time RT-PCR

Tissue RNA was isolated from homogenized hippocampus using RiboEX (Gene All, Seoul, Korea), and total RNA (0.2 μg) was reverse transcribed into cDNA according to the manufacturer's instructions using Applied Biosystems (Foster City, CA, USA). For the quantitative, real-time, reverse transcriptase polymerase chain reaction (PCR) assays, the linearity of the amplifications of CAPN1, CAPN2, NMDAR2A, NMDAR2B, Caspase-3, WIP1, BDNF,TP53, IL-1β, IL-6, TNF-α, and GAPDH cDNAs was established in preliminary experiments. All signal mRNAs were normalized to GAPDH mRNA. cDNAs were amplified by real-time PCR in duplicate with QuantiNova SYBR green PCR kit (Qiagen, Valencia, CA, USA). Each sample was run with the following primer sets: mCAPN1, 5'-GAGGCTGCAGGAACTACCC-3'(sense),5'-ATAGTCGTCTGCGTCATCCA-3'(antisense); mCAPN2, 5'-TCAGAAGGCTGTTTGCTCAG-3'(sense),5'-GCGCTTGGCTAGAACTCTTC-3'(antisense); mNMDAR2A, 5'-AGCCATTGCTGTCTTCGTTT-3'(sense),5'-ATCTTGCTGGTTGTGCCTTT-3'(antisense); mNMDAR2B, 5'-GCGATAATGGCGGATAAGGA-3'(sense),5'-AGGTAGGTGGTGACGATGGAA-3'(antisense); mCaspase-3,5'-CCTCAGAGAGACATTCATGG-3'(sense),5'-GCAGTAGTCGCCTCTGAAGA-3'(antisense);WIP1, BDNF,TP53,mIL-1β5'-TGCCACCTTTTGACAGTGATG-3'(sense),5'-ATGTGCTGCTGCGAGATTTG-3'(antisense);mIL-6,5'-CCACTTCACAAGTCGGAGGC-3'(sense),5'-GCCATTGCACAACTCTTTTCTCA-3'(antisense);mTNF-α, 5'-TGTAGCCCACGTCGTAGCAA-3'(sense),5'-

AGGTACAACCCATCGGCTGG-3'(antisense); mTP53, 5'-ACCGCCGACCTATCCTTACC-3' (sense), 5'-TCTTCTGTACGGCGGTCTCTC-3' (antisense);mGAPDH: 5'-AGGTCGGTGTGAACGGATTTG-3' (sense), 5'-TGTAGACCATGTAGTTGAGGTCA-3' (antisense).

Measurements of glutamate release

Homogenized tissue and PC12 cell supernatant samples were analyzed using the Shimadzu Prominence LC-20AD HPLC system equipped with an electrochemical detector Nanospace 3005 (OSAKA SODA, Tokyo, Japan) using a Unison UK-C18 column (IMTAKT, Kyoto, Japan; 2.0 mm × 50 mm). The graphite working electrode of the electrochemical detector was set at +850 mV with respect to an Ag/AgCl reference electrode. The mobile phase consisted of 50 mM phosphoric acid, 50 mM citric acid, 0.1 mM EDTA (pH 3.5), and 5% acetonitrile at a flow rate of 0.3 mL/min. For detection of 20 μL of sample was added to 2 μL of reactive solution prepared from o-phthaldialdehyde (37 mM) in 0.1 M borate buffer (pH 10.4) containing 250 μL ethanol and 50 mM sodium sulfite. The samples (10 μL) were then injected into the HPLC system. The amount of neurotransmitter in dialysate was calculated using the Labsolutions software (Shimadzu, Kyoto, Japan).

Cytokine Assay

Tissue levels of mouse TNF-α, IL-6, and IL-1β were measured by enzyme-linked immunosorbent assay (ELISA) kits provided by R&D systems (Minneapolis, MN, USA) according to the manufacturer's protocol.

Statistical Analysis

Data were analyzed by using GraphPad Prism v8.0. All data was examined for normal distribution with D'Agostino & Pearson normality test. If data set exhibited normal distribution, unpaired two-tailed student t test or two-way ANOVA for repeated measures and Bonferroni post-hoc analysis was used. If data set did not show normal distribution, two-tailed Mann-Whitney U test was used.

Declarations

Acknowledgements

We thank all the authors for feedback on the manuscript and fruitful discussions. This work is financially supported by the National Research Foundation of Korea [NRF] Grant funded by the Korea government (MSIP) (No. MRC, 2017R1A5A2015541).

Contributions

Jin Tae Hong, In Jun Yeo, Ji Eun Yu, and Sung Sik Yoo conceived the design of this study and coordinated all phases of the preparation of the manuscript. In Jun Yeo, Ji Eun Yu, Sung Sik Yoo, Jaesuk Yun, Dong Ju Son, Dong-Young Choi, Sang-Bae Han, and Jin Tae Hong participated in data analysis and helped draft the manuscript. All authors read and approved the final manuscript.

Competing Interests

The authors declare that they have no competing interest.

References

1 Driver, J. A. Inverse association between cancer and neurodegenerative disease: review of the epidemiologic and biological evidence. *Biogerontology***15**, 547-557 (2014).

2 Papin, S. & Paganetti, P. Emerging Evidences for an Implication of the Neurodegeneration-Associated Protein TAU in Cancer. *Brain Sciences***10**, 862 (2020).

3 Xiao, H. *et al.* Impact of comorbidities on prostate cancer stage at diagnosis in Florida. *American journal of men's health***10**, 285-295 (2016).

4 Snyder, H. M. *et al.* Exploring the nexus of Alzheimer's disease and related dementias with cancer and cancer therapies: A convening of the Alzheimer's Association & Alzheimer's Drug Discovery Foundation. *Alzheimer's & Dementia***13**, 267-273 (2017).

5 Zuber, V. *et al.* Identification of shared genetic variants between schizophrenia and lung cancer. *Scientific reports***8**, 1-8 (2018).

6 Nakanishi, A., Minami, A., Kitagishi, Y., Ogura, Y. & Matsuda, S. BRCA1 and p53 tumor suppressor molecules in Alzheimer's disease. *International journal of molecular sciences***16**, 2879-2892 (2015).

7 Guo, X. *et al.* Inhibition of mitochondrial fragmentation diminishes Huntington's disease–associated neurodegeneration. *The Journal of clinical investigation***123**, 5371-5388 (2013).

8 Jembrek, M. J., Slade, N., Hof, P. R. & Šimić, G. The interactions of p53 with tau and Aß as potential therapeutic targets for Alzheimer's disease. *Progress in neurobiology***168**, 104-127 (2018).

9 Campbell, W. A. *et al.* Zebrafish lacking Alzheimer presenilin enhancer 2 (Pen-2) demonstrate excessive p53-dependent apoptosis and neuronal loss. *Journal of neurochemistry***96**, 1423-1440 (2006).

10 Gandhi, S. & Wood, N. W. Molecular pathogenesis of Parkinson's disease. *Human molecular genetics***14**, 2749-2755 (2005).

11 Aubrey, B. J., Kelly, G. L., Janic, A., Herold, M. J. & Strasser, A. How does p53 induce apoptosis and how does this relate to p53-mediated tumour suppression? *Cell Death & Differentiation***25**, 104-113 (2018).

12 Kung, C.-P. & Murphy, M. E. The role of the p53 tumor suppressor in metabolism and diabetes. *The Journal of endocrinology***231**, R61 (2016).

13 Zhang, C.-g., Wan, H.-q., Ma, K.-n., Luan, S.-x. & Li, H. Identification of biomarkers related to neuropathic pain induced by peripheral nerve injury. *Journal of Molecular Neuroscience***69**, 505-515 (2019).

14 Szybińska, A. & Leśniak, W. P53 dysfunction in neurodegenerative diseases-the cause or effect of pathological changes? *Aging and disease***8**, 506 (2017).

15 Catts, V. S. *et al.* Apoptosis and schizophrenia: a pilot study based on dermal fibroblast cell lines. *Schizophrenia research***84**, 20-28 (2006).

16 Gassó, P. *et al.* Increased susceptibility to apoptosis in cultured fibroblasts from antipsychotic-naïve first-episode schizophrenia patients. *Journal of psychiatric research***48**, 94-101 (2014).

17 Ma, X., Fei, E., Fu, C., Ren, H. & Wang, G. Dysbindin-1, a schizophrenia-related protein, facilitates neurite outgrowth by promoting the transcriptional activity of p53. *Molecular psychiatry***16**, 1105-1116 (2011).

18 Mao, X. *et al.* The tricyclic antidepressant amitriptyline inhibits D-cyclin transactivation and induces myeloma cell apoptosis by inhibiting histone deacetylases: in vitro and in silico evidence. *Molecular pharmacology***79**, 672-680 (2011).

19 Angelucci, F., Brene, S. & Mathe, A. BDNF in schizophrenia, depression and corresponding animal models. *Molecular psychiatry***10**, 345-352 (2005).

20 Huang, H.-J. *et al.* Ghrelin alleviates anxiety-and depression-like behaviors induced by chronic unpredictable mild stress in rodents. *Behavioural brain research***326**, 33-43 (2017).

21 Ruan, C. S. *et al.* Mice deficient for wild-type p53-induced phosphatase 1 display elevated anxiety-and depression-like behaviors. *Neuroscience***293**, 12-22 (2015).

22 Baudry, M. Calpain-1 and Calpain-2 in the Brain: Dr. Jekill and Mr Hyde? *Current neuropharmacology***17**, 823-829 (2019).

23 Martin, H. G. & Wang, Y. T. Blocking the deadly effects of the NMDA receptor in stroke. *Cell***140**, 174-176 (2010).

24 Alsabban, A. H., Morikawa, M., Tanaka, Y., Takei, Y. & Hirokawa, N. Kinesin Kif3b mutation reduces NMDAR subunit NR 2A trafficking and causes schizophrenia-like phenotypes in mice. *The EMBO journal***39**, e101090 (2020).

25 Woo, T.-U. W., Shrestha, K., Lamb, D., Minns, M. M. & Benes, F. M. N-methyl-D-aspartate receptor and calbindin-containing neurons in the anterior cingulate cortex in schizophrenia and bipolar disorder. *Biological psychiatry***64**, 803-809 (2008).

26 Merlo, P. *et al.* p53 prevents neurodegeneration by regulating synaptic genes. *Proceedings of the National Academy of Sciences***111**, 18055-18060 (2014).

27 Turnquist, C. *et al.* p53 isoforms regulate astrocyte-mediated neuroprotection and neurodegeneration. *Cell Death & Differentiation***23**, 1515-1528 (2016).

28 Morrison, R. & Kinoshita, Y. The role of p53 in neuronal cell death. *Cell Death & Differentiation***7**, 868-879 (2000).

29 Biswas, S. C., Ryu, E., Park, C., Malagelada, C. & Greene, L. A. Puma and p53 play required roles in death evoked in a cellular model of Parkinson disease. *Neurochemical research***30**, 839-845 (2005).

30 Vesce, S., Rossi, D., Brambilla, L. & Volterra, A. Glutamate release from astrocytes in physiological conditions and in neurodegenerative disorders characterized by neuroinflammation. *International review of neurobiology***82**, 57-71 (2007).

31 Harrison, P. J., Hall, N., Mould, A., Al-Juffali, N. & Tunbridge, E. M. Cellular calcium in bipolar disorder: systematic review and meta-analysis. *Molecular psychiatry*, 1-11 (2019).

32 Casamassima, F. *et al.* L-type calcium channels and psychiatric disorders: A brief review. *American Journal of Medical Genetics Part B: Neuropsychiatric Genetics***153**, 1373-1390 (2010).

33 Einat, H., Karbovski, H., Korik, J., Tsalah, D. & Belmaker, R. Inositol reduces depressive-like behaviors in two different animal models of depression. *Psychopharmacology***144**, 158-162 (1999).

34 Yamamoto, T. & Takahara, A. Recent updates of N-type calcium channel blockers with therapeutic potential for neuropathic pain and stroke. *Current topics in medicinal chemistry***9**, 377-395 (2009).

35 Terasaki, Y. *et al.* Activation of NR2A receptors induces ischemic tolerance through CREB signaling. *Journal of Cerebral Blood Flow & Metabolism***30**, 1441-1449 (2010).

36 Singh, A. K. *et al.* Neuroprotection through rapamycin-induced activation of autophagy and PI3K/Akt1/mTOR/CREB signaling against amyloid-β-induced oxidative stress, synaptic/neurotransmission dysfunction, and neurodegeneration in adult rats. *Molecular neurobiology***54**, 5815-5828 (2017).

37 Seinfeld, J., Baudry, N., Xu, X., Bi, X. & Baudry, M. Differential activation of calpain-1 and calpain-2 following kainate-induced seizure activity in rats and mice. *Eneuro***3** (2016).

38 Miao, Y. *et al.* Involvement of calpain/p35-p25/Cdk5/NMDAR signaling pathway in glutamate-induced neurotoxicity in cultured rat retinal neurons. (2012).

39 Almeida, R. *et al.* Neuroprotection by BDNF against glutamate-induced apoptotic cell death is mediated by ERK and PI3-kinase pathways. *Cell Death & Differentiation***12**, 1329-1343 (2005).

40 Dong, Y. *et al.* Involvement of Akt/CREB signaling pathways in the protective effect of EPA against interleukin-1β-induced cytotoxicity and BDNF down-regulation in cultured rat hippocampal neurons. *BMC neuroscience***19**, 1-8 (2018).

41 Zipp, F. & Aktas, O. The brain as a target of inflammation: common pathways link inflammatory and neurodegenerative diseases. *Trends in neurosciences***29**, 518-527 (2006).

42 Heneka, M. T. *et al.* Neuroinflammation in Alzheimer's disease. *The Lancet Neurology***14**, 388-405 (2015).

43 Lin, T. *et al.* Emerging roles of p53 related lncRNAs in cancer progression: a systematic review. *International journal of biological sciences***15**, 1287 (2019).

44 Hwang, C. J. *et al.* Reducing effect of IL-32α in the development of stroke through blocking of NF-κB, but enhancement of STAT3 pathways. *Molecular neurobiology***51**, 648-660 (2015).

Figures

Figure 1

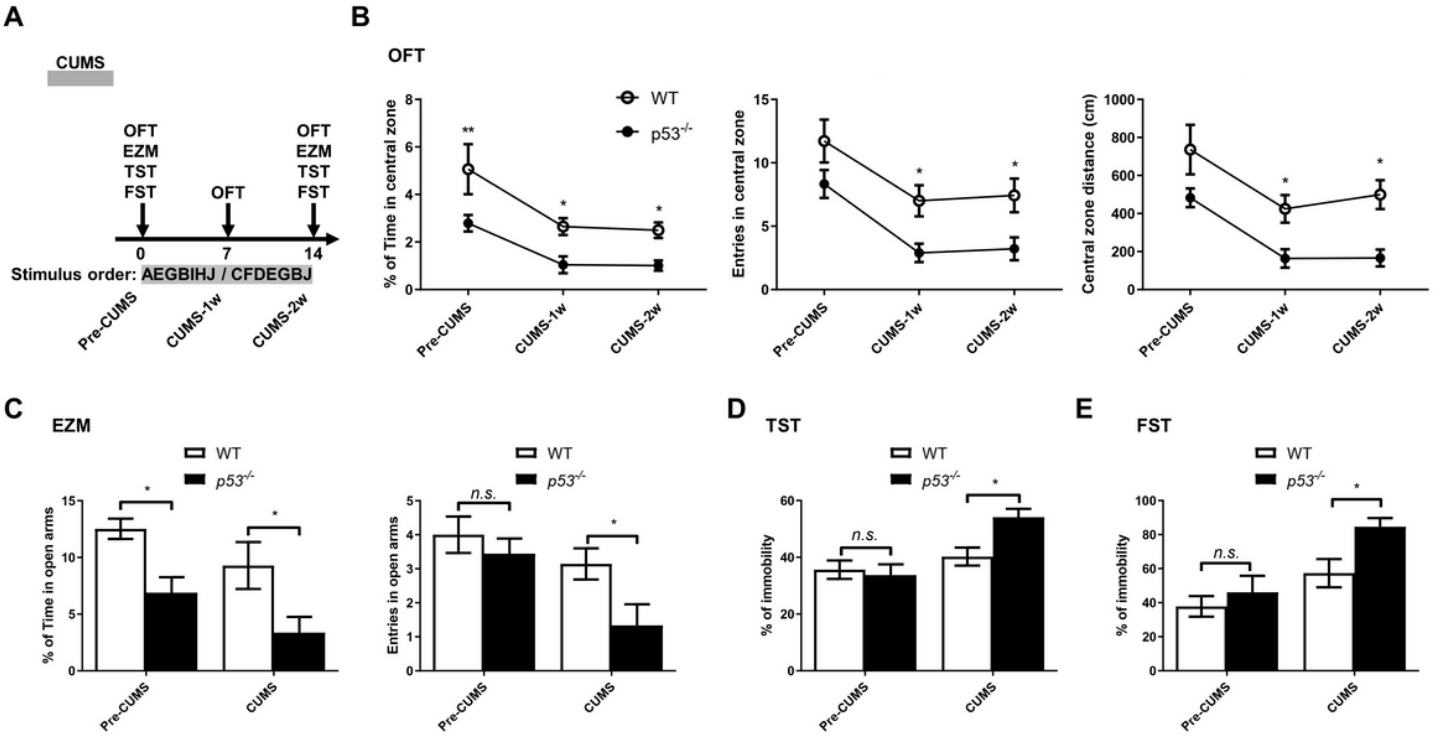

Figure 1

Timeline of CUMS stimulation and behavioral tests schedule (A). Locomotor activity and anxiety measured as time (in %), entries, and distance (in cm) in central zone in open field test (OFT) weekly during CUMS (B).Basal anxiety assessed as time (in %) and entries in open vs closed arms in the elevated zero maze (EZM) (C). Depression immobility time (in %) in tail suspension test (TST) (D) and forced swimming test (FST) (E). Data are represented as means± SEM (WT, n = 7; p53-/-,n= 9). *p<0.05 and **p<0.01 Significant difference from WT mice.

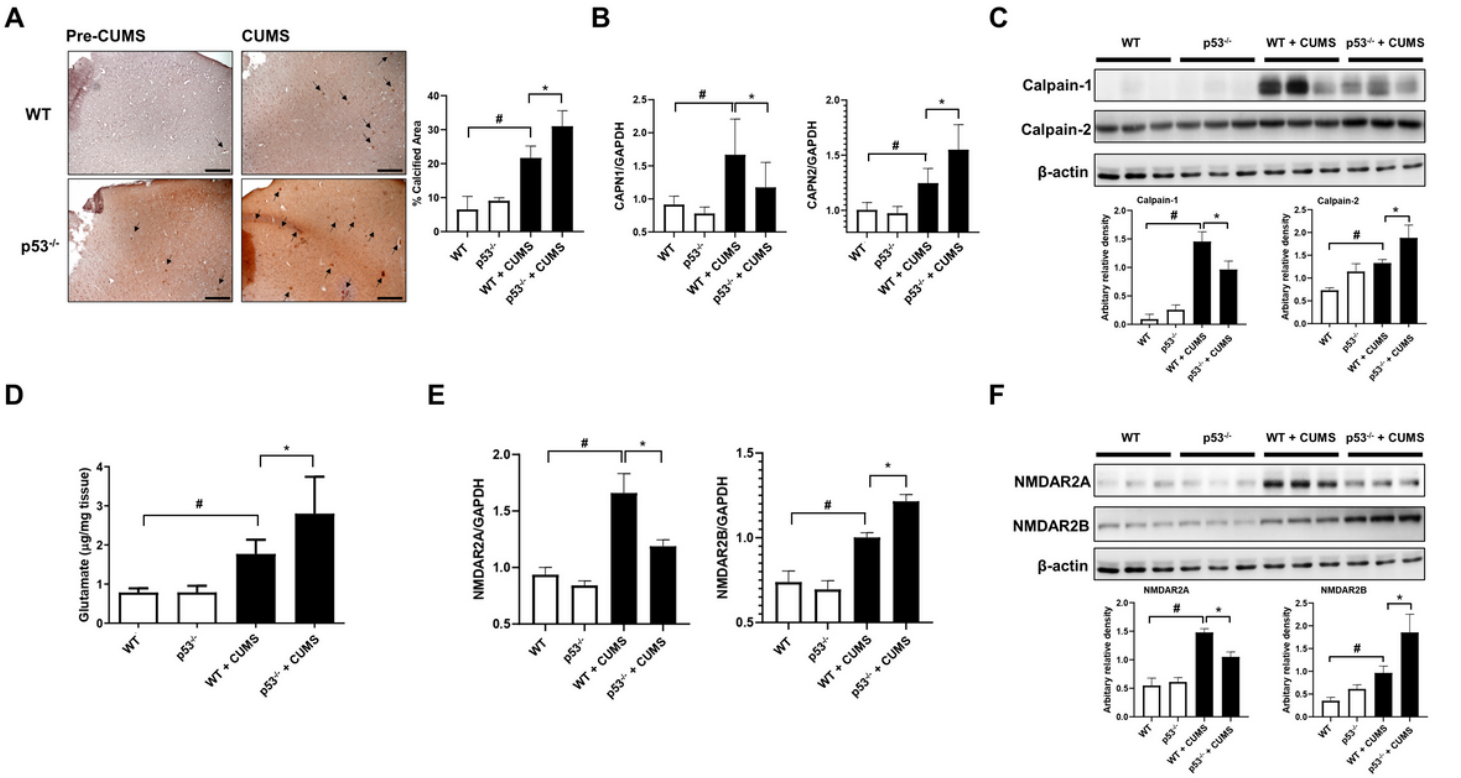

Figure 2

Calcium staining by alizarin red S in PFC, arrows indicate calcium-stained red spot (A). Scale bars represent 200 μm. The mRNA expression levels of CAPN1 and CAPN2 in PFC (B). The protein levels of calpain-1 and calpain-2 in PFC (C).The glutamate levels in homogenized PFC determined by HPLC-ECD (D). The mRNA expression levels of NMDAR2A and NMDAR2B in PFC (E). The protein levels of NMDAR2A and NMDAR2B in PFC (F).β-actin levels were measured to confirm equal protein loading. The values on the Western blot bands represent the arbitrary density measured by ImageJ.Data are represented as means± SEM from three mice brains. *p<0.05Significant difference from WT + CUMS mice and #p<0.05 Significant difference from WT mice.

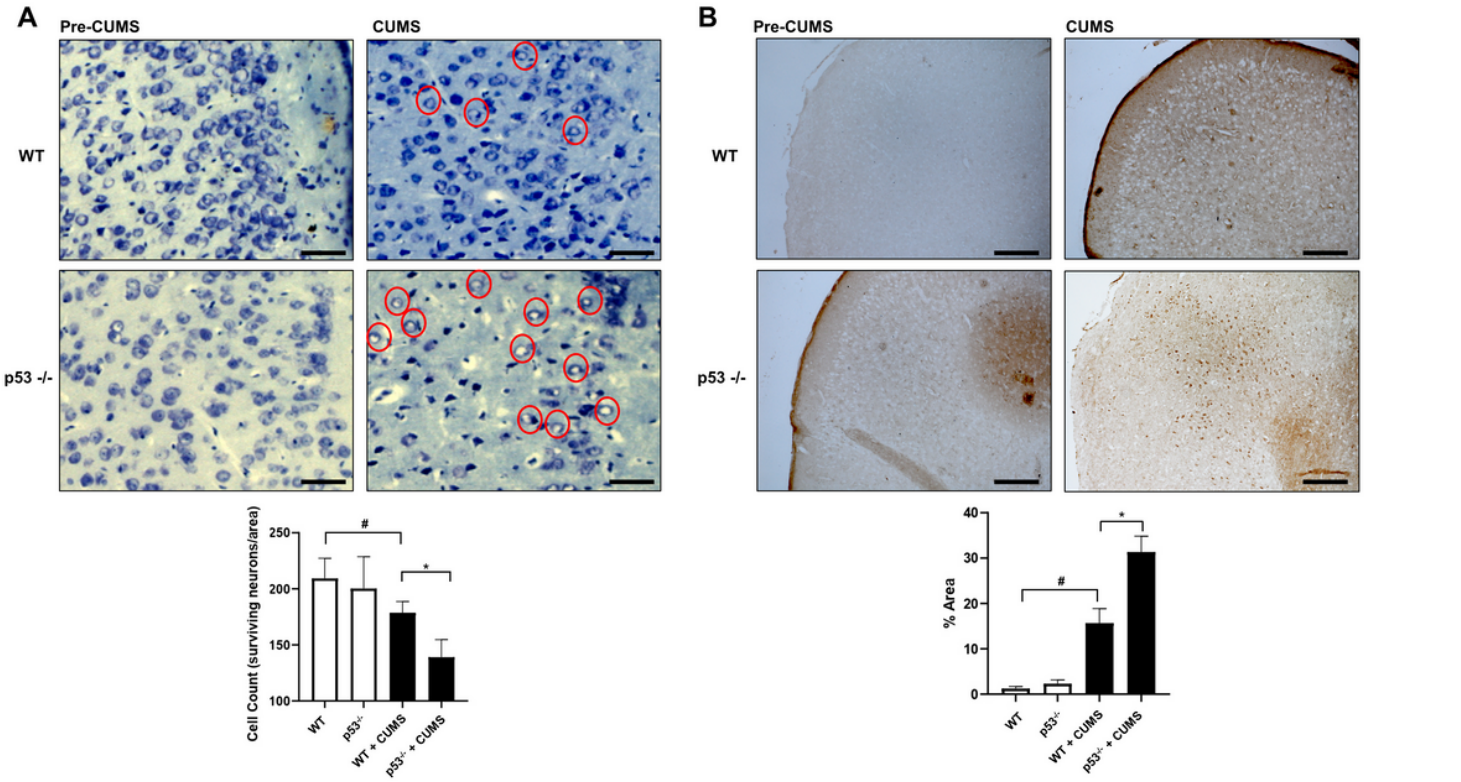

Figure 3

Cresyl violet staining in mice PFC, red circle indicates damaged neuronal cells (A). Scale bars represent 100 µm. Immunostaining of cleaved caspase-3 in PFC (B).Scale bars represent 200 µm. Data are represented as means± SEM from three mice brains.*p<0.05Significant difference from WT + CUMS mice and #p<0.05 Significant difference from WT mice.

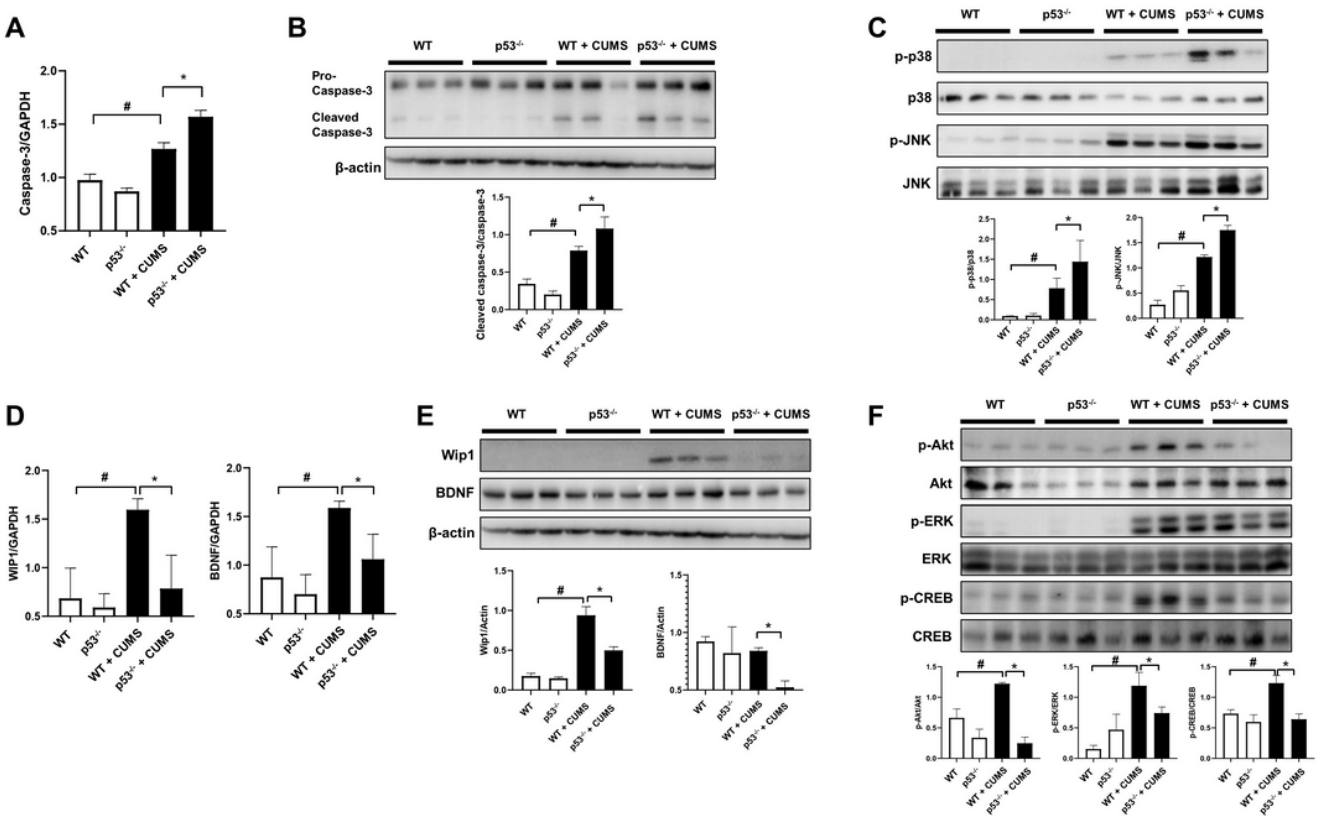

Figure 4

The mRNA expression levels of caspas3 in PFC (A). The protein levels of pro-caspase3 and cleaved caspase3 in PFC (B).p-p38, p38, p-JNK and JNK proteins were detected by Western blotting using specific antibodies in mice PFC (C). The mRNA expression levels of WIP1 and BDNF in PFC (D).Wip1 and BDNF proteins were detected by Western blotting using specific antibodies in mice PFC (E). p-Akt, Akt, p-ERK, ERK, p-CREB and CREB proteins were detected by Western blotting using specific antibodies in mice PFC (F). β-actin was internal control. The values on the Western blot bands represent the arbitrary density measured by ImageJ.Data are represented as means± SEM from three mice brains.*$p<0.05$Significant difference from WT + CUMS mice and #$p<0.05$ Significant difference from WT mice.

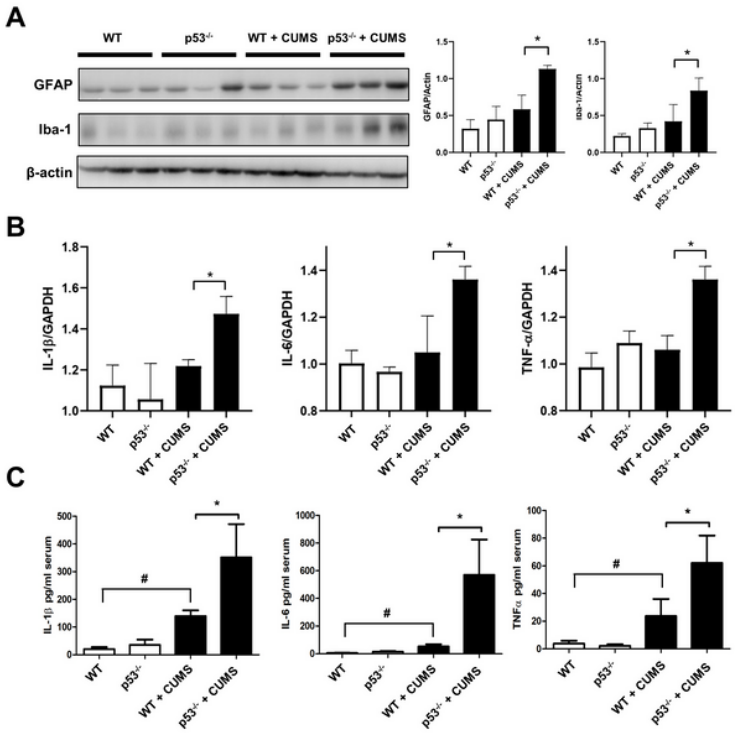

Figure 5

The expression levels of GFAP and Iba-1in the mice PFC were detected by Western blotting using specific antibodies.β-actin levels were measured to confirm equal protein loading. The values on the Western blot bands and graph represent the arbitrary density measured by ImageJ(A). The mRNA levels of IL-1β, IL-6, andTNF-α were detected by qRT-PCR in mice PFC (B). The protein levels of IL-1β, IL-6, andTNF-α were detected by ELISA in mice serum.Data are represented as means± SEM from three mice brains.*p<0.05Significant difference from WT + CUMS mice and #p<0.05 Significant difference from WT mice.

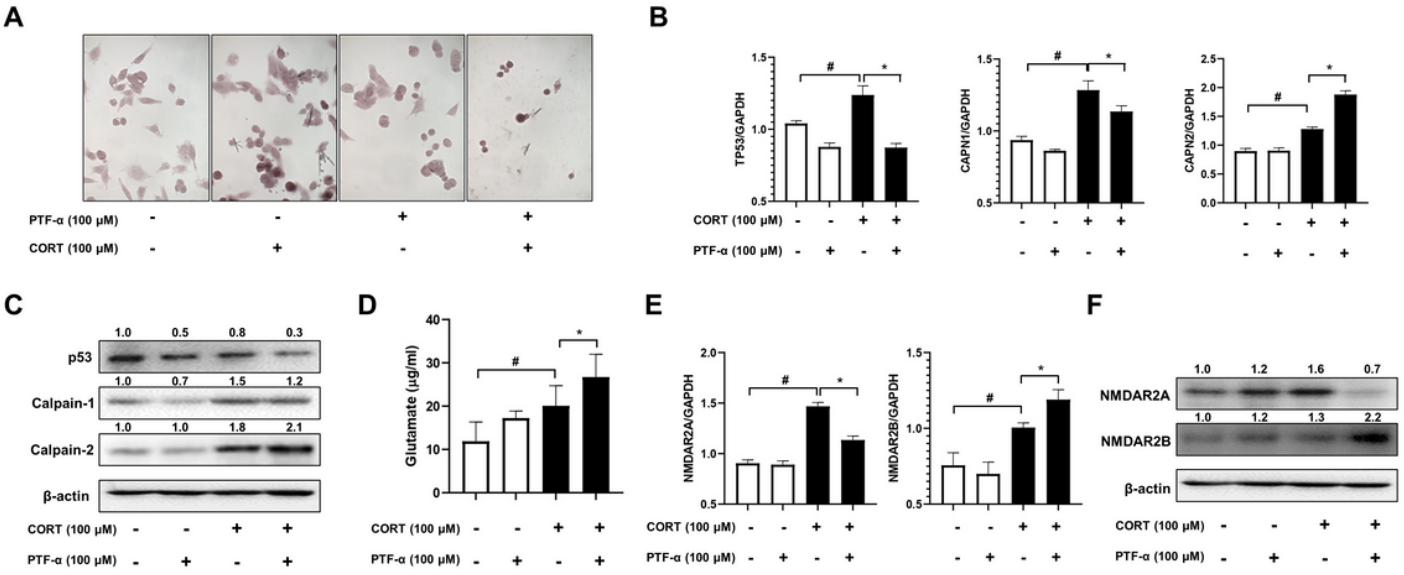

Figure 6

Effect of p53 inhibitor (PTF-α) on the CUMS mimic stimulation by corticosterone (CORT) treatmentinPC12 cells. PC12 cells were treatedwith CORT and treated for 24 hours with or without PTF-α. Calcium staining by Alizarin red S and cell density of PC12 cells (A).The mRNA levels of TP53, CAPN1, andCAPN2 were detected by qRT-PCR in PC12 cells (B).The protein expression of p53, calpain-1, andcalpain-2 were detected by Western blotting using specific antibodies (C).The glutamate levels in PC12 cells supernatant by HPLC-ECD (D). The mRNA levels of NMDAR2A andNMDAR2B were detected by qRT-PCR in PC12 cells (E).The protein expression of NMDAR2A andNMDAR2B were detected by Western blotting using specific antibodies (F).The experiment was performed in triplicate. β-actin levels were measured to confirm equal protein loading. The values on the Western blot bands and graph represent the arbitrary density measured by ImageJ.Data are represented as means± SEM (n = 3).*p<0.05Significant difference from CORT treated PC12 cells and #p<0.05 Significant difference from non-treated PC12 cells.

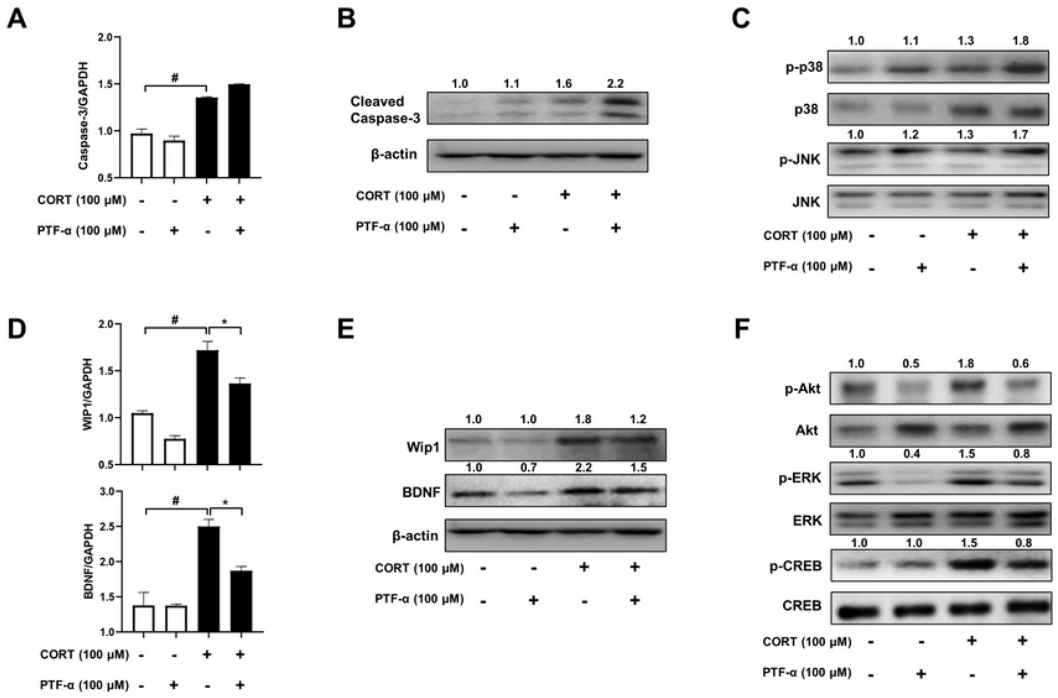

Figure 7

Effect of p53 inhibitor (PTF-α) on the CUMS mimic stimulation by corticosterone (CORT) treatmentinPC12 cells. PC12 cells were treatedwith CORT and treated for 24 hours with or without PTF-α. The mRNA expression levels of caspase-3 in PC12 cells(A). The protein levels of caspase-3 in PC12 cells (B).p-p38, p38, p-JNK and JNK proteins were detected by Western blotting using specific antibodies in PC12 cells (C). The mRNA expression levels of WIP1 and BDNF in PC12 cells(D).Wip1 and BDNF proteins were detected by Western blotting using specific antibodies in PC12 cells (E). p-Akt, Akt, p-ERK, ERK, p-CREB and CREB proteins were detected by Western blotting using specific antibodies in PC12 cells (F). β-actin was internal control.All experiments were performed three times with duplicate. The values on the Western blot bands represent the arbitrary density measured by ImageJ.Data are represented as means± SEM (n = 3).*p<0.05Significant difference from CORT treated PC12 cells and #p<0.05 Significant difference from non-treated PC12 cells.

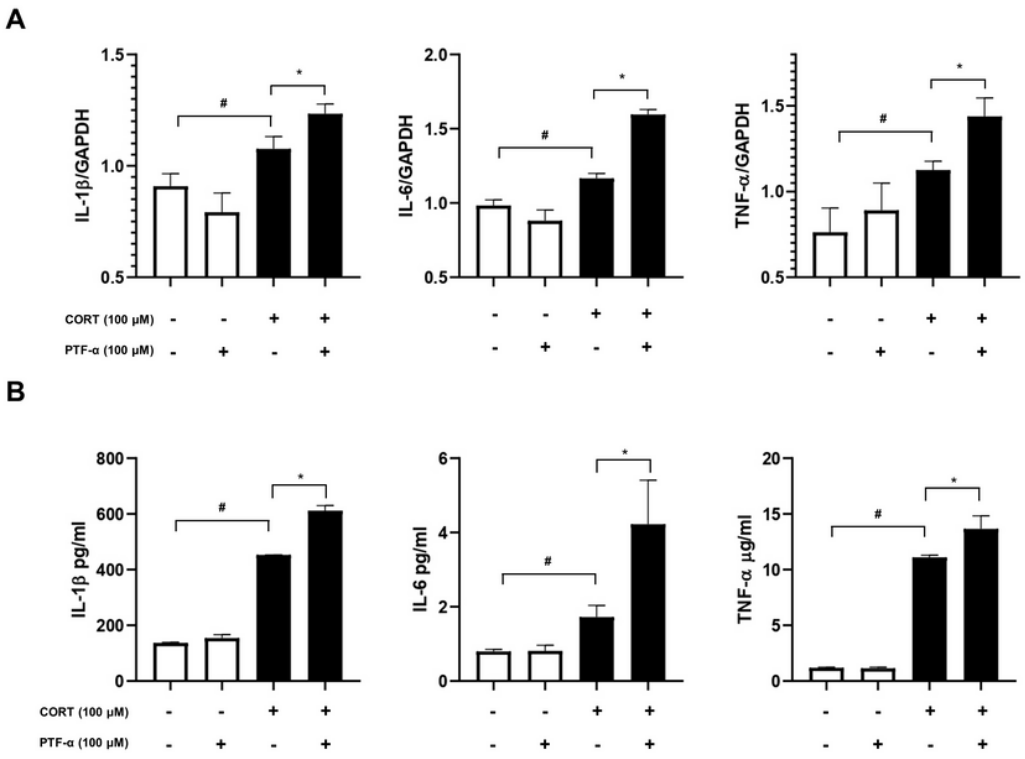

Figure 8

The mRNA levels of IL-1β, IL-6, andTNF-α were detected by qRT-PCR in PC12 cells (A). The protein levels of IL-1β, IL-6, andTNF-α were detected by ELISA in PC12 cells supernatant (B). All experiments were performed three times with duplicate.Data are represented as means± SEM (n = 3). *p<0.05Significant difference from CORT treated PC12 cells and #p<0.05 Significant difference from non-treated PC12 cells.

Supplementary Files

This is a list of supplementary files associated with this preprint. Click to download.

- SupplementaryFigure1.tif
- SupplementaryFigure2.tif
- SupplementaryFigure3.tif
- SupplementaryFigure4.tif
- SupplementaryFigurelegends.docx